Fracture Toughness Measurements of Two Specimen Geometries Considering Stability in Brittle Materials

Kyu Cho
Francis I. Baratta (retired)
U.S. ARMY RESEARCH LABORATORY

Isa Bar-On
WORCESTER POLYTECHNIC INSTITUTE

19960913 155

NOTICES

REPORT DOCUMENTATION PAGE

1. AGENCY USE ONLY (Leave blank)	2. REPORT DATE	3. REPORT TYPE AND DATES COVERED
	August 1996	Final, Apr 94 - Sep 95

4. TITLE AND SUBTITLE
Fracture Toughness Measurements of Two Specimen Geometries Considering Stability in Brittle Materials

5. FUNDING NUMBERS
4CL00R3L44LAL
4CL00X2L24L02
5S2LBA

6. AUTHOR(S)

Kyu Cho, Francis I. Baratta, and Isa Bar-On*

7. PERFORMING ORGANIZATION NAME(S) AND ADDRESS(ES)

U.S. Army Research Laboratory
ATTN: AMSRL-MA-I
Aberdeen Proving Ground, MD 21005-5069

8. PERFORMING ORGANIZATION REPORT NUMBER

ARL-TR-1184

9. SPONSORING/MONITORING AGENCY NAMES(S) AND ADDRESS(ES)

10. SPONSORING/MONITORING AGENCY REPORT NUMBER

11. SUPPLEMENTARY NOTES
*Worcester Polytechnic Institute

12a. DISTRIBUTION/AVAILABILITY STATEMENT

Approved for public release; distribution is unlimited.

12b. DISTRIBUTION CODE

13. ABSTRACT (Maximum 200 words)

It has been shown that a lack of stable crack extension can influence the critical stress intensity factor (SIF) measured for brittle materials. Previously performed stability analyses of two specimen geometries were used to design experiments, which would make it possible to observe the transition from unstable to stable fracture as a function of the specimen compliance. This transition was observed to be in agreement with the predictions. The lack of stability gave higher critical SIF values for the material with the higher fracture toughness, while this difference was lost in the experimental scatter for the other materials.

14. SUBJECT TERMS

fracture toughness, crack stability, brittle materials

15. NUMBER OF PAGES
21

16. PRICE CODE

17. SECURITY CLASSIFICATION OF REPORT	18. SECURITY CLASSIFICATION OF THIS PAGE	19. SECURITY CLASSIFICATION OF ABSTRACT	20. LIMITATION OF ABSTRACT
			UL

INTENTIONALLY LEFT BLANK.

ACKNOWLEDGMENTS

INTENTIONALLY LEFT BLANK.

TABLE OF CONTENTS

INTENTIONALLY LEFT BLANK.

LIST OF FIGURES

INTENTIONALLY LEFT BLANK.

LIST OF TABLES

INTENTIONALLY LEFT BLANK.

1. INTRODUCTION

Fracture toughness of metallic materials is typically determined at the start of quasi-static crack extension (Srawley and Brown 1966). The quasi-static condition is achieved during fracture by the low rate of increase in stress intensity, 0.55 to 2.75 $MPa\sqrt{m}/s$ (ASTM E-399 1989). In addition, the quasi-static extension is aided or even facilitated by local crack tip plasticity in these materials.

For ceramic materials, however, quasi-static crack extension is much more difficult to obtain. These inherently brittle materials do not benefit from the crack tip plastic zone. Also, fracture toughness tests in ceramics are typically performed at higher loading rates in order to avoid the effect of potential environmental interactions with the grain boundary phase. At low loading rates, this interaction can lead to artificially low fracture toughness measurements (Fett and Munz 1993; Nose and Fujii 1987).

The lack of quasi-static or stable crack extension has been recognized to affect fracture testing even for relatively ductile materials (Clausing 1969). Unstable fracture as encountered, for example, in notched specimen tests will frequently lead to artificially high fracture toughness values. Similarly, unstable fracture tends to occur in very stiff specimens, such as ceramics, when the test setup is not sufficiently stiff relative to the specimen. For those materials, crack stability is often extremely difficult to obtain even for specimens containing naturally sharp cracks. Underwood, Baratta, and Zalinka (1991) and Baratta and Dunlay (1990) have shown that this lack of stability can lead to inflated critical stress intensity factor (SIF) measurements for liquid-phase sintered tungsten and polymethylmethacrylate (PMMA) materials, respectively.

Baratta and Dunlay (1990) analyzed the crack stability of the rectangular bend bar (RTBB) in three-point and four-point loading. Their analysis and test results for quasi-brittle specimens showed that the three-point loading geometry had greater stability potential than the four-point loading geometry. Underwood, Baratta, and Zalinka (1991) analyzed the crack stability of a round bend bar (RBB). Their analysis and test results for tungsten specimens showed that the round bend bar specimen to be significantly more stable than the RTBB loading configuration. This would make the RBB specimen geometry an attractive candidate for fracture toughness testing of ceramic materials as it might promote stability in this case.

1

In ceramic materials, however, it is difficult to create sharp precracks in a reproducible and controllable manner. Recently a precracking method has been developed (Nose and Fujii 1988) and systematically studied (Bar-On et al. 1990) by which cracks of varying lengths can be introduced in RTBB specimens. For this method, a Vickers micro-indentation is placed on one of the specimen's longitudinal surfaces. A through thickness straight crack is then created by loading the specimen in compression between a double anvil fixture. This bridge indentation method (Warren and Johanneson 1969) can be applied to the RBB only if the cross section of the bar is modified to create two parallel, flat surfaces as shown in Figure 1. Cho, Hantz, and Bar-On (1993) modified the RBB specimen geometry to allow precracking while obtaining potentially greater crack stability. This new specimen geometry has been called the modified round bend bar (MRBB). Crack stability of the MRBB has been analyzed and compared to that of the RBB and RTBB Cho and Bar-On (1995).
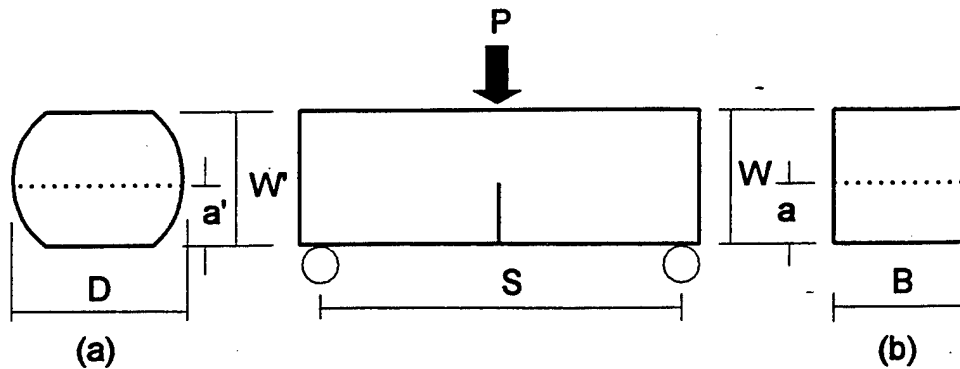
Figure 1. <u>Geometries of (a) the modified round bend bar (MRBB) and (b) the rectangular bend bar (RTBB)</u>.

As previously mentioned, recent works (Underwood, Baratta, and Zalinka 1991; Baratta and Dunlay 1990; Bar-On, Baratta, and Cho, to be published) have shown that unstable crack extension can result in an apparent increase in critical SIFs compared to those measured during stable crack growth of quasi-brittle polymer and brittle metallic materials. For both materials, the transition from stable to unstable fracture behavior was predicted based on stability analyses. The effect of crack stability on measured fracture toughness of ceramics, however, is unclear. Therefore, the objective of this work is the determination of the fracture toughness of ceramic materials while focusing on crack stability. The analytical stability prediction is compared to the fracture behavior observed for RTBB and MRBB

2

specimens of alumina and silicon nitride. The experimental results were in excellent agreement with the analytical prediction. Critical SIF measurements suggested that it would be necessary to select a material with a relatively high fracture toughness and a specimen with larger dimensions to observe a noticeable difference in critical SIFs due to crack instability. Also, it was predicted that stability in the MRBB can be obtained for shorter crack lengths than for the RTBB.

2. STABILITY SUMMARY

The stability equation for bend bars has been derived previously (Underwood, Baratta, and Zalinka 1991; Baratta and Dunlay 1990; Cho and Bar-On 1995) and is based on the requirement that at fracture:

$$dG \: / \: dA \leq dG_{CR} \: / \: dA, \tag{1}$$

where G is the elastic strain release rate, A is the crack face area, and G_{CR} is the critical elastic strain release rate. For materials with a flat crack growth resistance curve (i.e., $dG \: / \: dA = 0$), then Equation (1) becomes:

$$dG \: / \: dA \leq 0. \tag{2}$$

Bluhm (1977) has shown that stability for beams can be obtained for displacement control (i.e., fixed grip) conditions only. The stability equation for this condition is:

$$dG \: / \: dA = 1/2 \: \{P^2 \: (d^2\lambda_T \: / \: dA^2) + 2P \: (dP \: / \: dA) \: (d\lambda_T \: / \: dA)\} \leq 0$$

$$= G \: \{d^2\lambda_T \: / \: dA^2 - 2 \: / \: \lambda_T \: (d\lambda_T \: / \: dA)^2\} \: d\lambda_T \: / \: dA \leq 0, \tag{3}$$

where λ_T is the total compliance of the system consisting of the specimen compliance, λ_S, and that of the machine (including ancillary fixture, λ_M), and P is the applied load.

The nondimensional load-line compliance for the cracked RTBB and MRBB is taken from the literature (Cho and Bar-On 1995; Baratta 1988). For the RTBB, the nondimensional, plain strain compliance, $\overline{\lambda}_{RTBB} = (\delta EB \: / \: P)_{RTBB}$, is:

$$\bar{\lambda}_{RTBB} = 2\,(S/2W)^2\,[S/2W + \{2.85\,/\,(S/2W) - 0.42\,/\,(S/2W)^2\}$$

$$/\,4 + 9\,(1 + v^2)\int \alpha\,f^2(\alpha)\,d\alpha], \tag{4}$$

where δ, E, P, B, S, W, and are the load-line deflection, the elastic modulus, the applied load, the specimen thickness, the span length, the width of the specimen, Poisson's ratio, and the dimensionless crack length, respectively (Baratta 1988). $f(\alpha)$ (Bar-On, Baratta, and Cho, to be published; Srawley 1976; Brown and Srawley 1966) is the dimensionless stress intensity factor expression for the RTBB. For the MRBB, the nondimensional plain strain compliance, $\bar{\lambda}_{MRBB} = (\delta ED\,/\,P)_{MRBB}$, is:

$$\bar{\lambda}_{MRBB} = (S/W')^3\,\{3.4862 \times 10^{-1} + 8.0862 \times 10^{-1}\,(1 + v)\,/\,(S/W')^2\}$$

$$+ 2.2992\,(S/W')^2\,/\,W'^2\,[\alpha'\,f^2(\alpha')\,g(\alpha')\,/\,\{(1 - \alpha')^3\,(\Omega + 1 - \alpha')\}]\,d\alpha', \tag{5}$$

where D, W', and α' are the diameter, the width, and the dimensionless crack length of the MRBB, respectively (Cho and Bar-On 1995). $f(\alpha')$ (Cho, Hantz, and Bar-On 1993) is the dimensionless stress intensity factor for the MRBB. $g(\alpha') = dA\,/\,d\alpha'$ (Cho and Bar-On 1995), and Ω (Cho, Hantz, and Bar-On 1993) are geometry constants for the MRBB.

The stability solution for the RTBB and MRBB in the three-point bending can be derived using the nondimensional machine compliance, $\bar{\lambda}_M = \delta_M EB/P$ for the RTBB and $\bar{\lambda}_M = \delta_M ED/P$ for the MRBB, respectively. The results of the stability calculation relevant for the experiments are summarized in Figure 2 in terms of threshold crack length. The threshold crack length is the minimum nondimensional crack length for which stable crack growth can be predicted. Nondimensional machine compliance, including test fixture and span-to-width ratios used in the experimental tests, were $\bar{\lambda}_M \approx 60$ (see experimental procedure for detailed description), and S/W = 5 for the RTBB and S/W' = 6 and 6.25 for the MRBB, respectively.
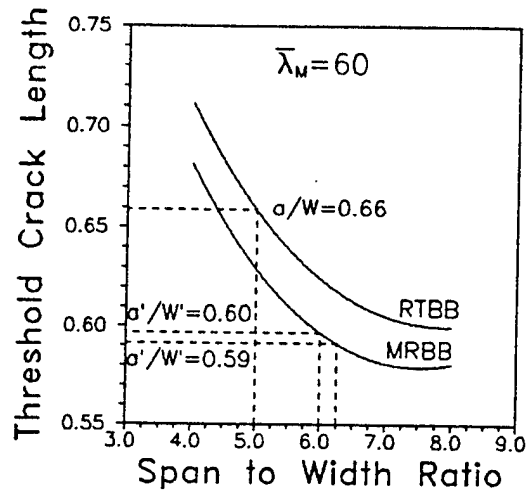
Figure 2. <u>The threshold crack length for the rectangular and modified round bend bars with a nondimensional machine compliance, $\overline{\lambda}_M$, of 60.</u>

3. EXPERIMENTAL PROCEDURE

The RTBB and MRBB geometries were used to measure fracture toughness of an alumina (AD99*) and silicon nitride (NC132** and HS130**). Table 1 summarizes the mechanical and physical properties of the materials. The alumina was a Coors grade AD99 and was manufactured in the early to mid 1970s. AD99 is a nominally 99% Al_2O_3 with SiO_2 as a sintering additive. The average grain size is 12 μm (range of 2 to 50 μm) and the density is 3.83 g/cm^3 as reported by the manufacturer. A comparison of the theoretical density for 99% Al_2O_3 with the 3.83 g/cm^3 reported for AD99 suggests that a considerable amount of porosity can be expected. AD99 was primarily used as refractory thermocouples and electrical insulators. It had been extruded and then fabricated into a rod of 6.35 mm diameter. The rods were cut into 50-mm-long MRBB specimens with a D/W′ ratio of 1.1346 as shown in Figure 1.

One of the silicon nitride was a Norton grade HS130 (later developed into NC132) and was manufactured in the early to mid 1970s. HS130 is a nominally 98% pure Si_3N_4 utilizing MgO as a sintering agent. The major crystalline phase is β-Si_3N_4 and traces of α–Si_3N_4 and Si_2N_2O were identified

---

*   Coors Ceramics Co., Golden, CO.

** Norton Co., Worcester, MA.

Table 1. Mechanical and Physical Properties of AD99, NC132, and HS130

	Grain Size μm (range)	Density g/cm³ (range)	Elastic Modulus (GPa)	Poisson's Ratio	Modulus of Rupture (MPa)
AD99[a]	12 (2–50)[b]	3.83[c]	350[b]	0.24[c]	262[c]
NC132[d]	Maximum 3[e]	3.25[e]	320[e]	0.27[e]	825[e]
HS130[d]	2.5 (1–10)[f,g,h]	3.17–3.21[f]	300[f,g]	0.26–0.27[f]	516–681[f,g,i]

[a] Coors Ceramics, Golden, CO.
[b] Coors product literature.
[c] Quinn, Corbin, and McCauley (1994).
[d] Norton Co., Worcester, MA.
[e] Norton product literature.
[f] Miller et al. (1976).
[g] Bratton and Miller (1978).
[h] Lange and Iskoe (1974).
[i] Kossowsky (1974).

by x-ray diffraction (Miller et al. 1976). Three types of grains had been reported in the literature (Miller et al. 1976; Bratton and Miller 1978; Lange and Iskoe 1974): equiaxed grains ranging from 1 to 4 μm in size; equiaxed grains of the order of 8 to 10 μm; and elongated grains of 2 × 10 μm. A density of 3.17 to 3.21 g/cm³ has been reported (Miller et al. 1976) while that of NC132 is reported by the manufacturer as 3.25 g/cm³. This suggests that HS130 contains some porosity. The only measurement of this, however, consists of occasional layered shading of the x-ray radiographs (Miller et al. 1976; Kossowsky 1974). The comparatively wide range in density values is due to tungsten contaminations in the form of either WC or WSi_2. The mechanical properties are anisotropic due to the hot-pressing process. The modulus of rupture ranges from 516 to 681 MPa, the elastic modulus is 3.0×10^5 MPa, and Poisson's ratio is 0.26–0.27 (Miller et al. 1976; Bratton and Miller 1978; Kossowsky 1974). This is primarily a high-strength, high-temperature silicon nitride. The material was machined into 5.52-mm-diameter rods from 6 × 6 × 1½-in billets. The rods were cut into 50-mm-long MRBB specimens with a D/W' ratio of 1.1346. The silicon nitride used for the RTBB geometry fracture toughness tests was a Norton grade NC132. NC132 is a 100% theoretically dense, hot-pressed silicon nitride also using MgO as a sintering agent. The α-Si_3N_4/β-Si_3N_4 phase composition ratio is 20/80 (Ritter et al. 1988). The material has a maximum grain size of 3 μm. A density of 3.25 g/cm³, modulus of rupture of 825 ±137 MPa, Vickers hardness of 16 GPa, elastic modulus of 320 GPa, and Poisson's ratio of 0.27 have been reported by the

manufacturer. The material was cut into 6 × 8 × 45-mm RTBB specimens from 6 × 6 × 1-in billets with the hot pressing direction perpendicular both to the long direction of the specimen and to the crack plane.

The stability calculations were used as a guideline in designing a test system that would be stiff enough so that stable and unstable crack growth could be realized. The testing system consists of an Instron 250-kN servo-hydraulic load frame with a 25-kN load cell. Frame stiffness of 585 kN/mm, 250-kN capacity load cell stiffness of 2,560 kN/mm, and 25-kN capacity load cell stiffness of 1,020 kN/mm were all specified by the manufacturer. The resulting stiffness of the frame and the two load cells can be calculated as 322 kN/mm. Initially, a conventional, fully articulating, three-point bend test fixture, similar to the one specified in MIL-STD 1942A (1983), was used. With this setup, however, stable crack growth was unattainable even for very long precracks. The stability solution, which provided guidance to the experiments, indicated that the fixture had to be stiffened for stability to be obtained in this system. Thus, the fixture was replaced by a stiffer semiarticulating one. The compliance of the machine, load cells, and test fixture was determined experimentally using an uncracked silicon nitride bend bar. The measured compliance of this test setup was 3.07×10^{-8} m/N, corresponding to a stiffness of 32.57 kN/mm. This measured compliance corresponds to a nondimensional machine compliance of $\bar{\lambda}_M = 58.94$.

The specimens were indented with a Vickers diamond indenter using loads ranging from 69 to 490 N. Indentation was performed on a screw-driven Instron 5-kN load capacity testing machine with a 0.5-kN load cell at a displacement rate of 0.1 mm/min. The indenter was immediately released after the set loads had been reached. These specimens were precracked to dimensionless crack lengths of 0.2–0.8 a/W using the bridge indentation technique (Warren and Johanneson 1969). Precracking was performed on a servo-hydraulic Instron 250-kN capacity testing machine using a 25-kN load cell at a loading rate of 1 kN/s. The cracks were marked with dye penetrant ink, which was dried in a furnace after precracking. Crack length was measured after the test on the fracture surface at three equidistant points along the crack front (ASTM E-399 1989).

The fracture toughness tests were performed in three-point bending with three different span-to-width ratios: the span-to-width ratio for the RTBB was 5, for the MRBB, 6.25 for the alumina, and 6 for the silicon nitride specimens. The tests were performed on a servo-hydraulic Instron 250-kN capacity testing machine using a 25-kN load cell. The scale was set to 1/64 of full range. The fracture toughness tests were performed at a displacement rate of 0.1 mm/min for all materials. Two additional displacement rates

of 0.25 and 0.5 mm/min were used for the alumina, since alumina tends to be sensitive to subcritical crack growth in air (i.e., static fatigue) (Fett and Munz 1993). Load displacement records were taken for all tests.

4. RESULTS

The load displacement records showed three distinctly different traces. For initial critical crack lengths much less than the threshold value, the load displacement record was linear to the point of fracture as shown in Figure 3a. Fracture occurred instantaneously across the entire cross section as indicated by the load drop to zero. For initial critical crack lengths close to the critical crack length, some stable crack extension occurred as documented by the load displacement curves, which were nonlinear near the maximum load (see Figure 3b). Specimens with very long cracks exhibited more pronounced nonlinear load displacement records (see Figure 3c).
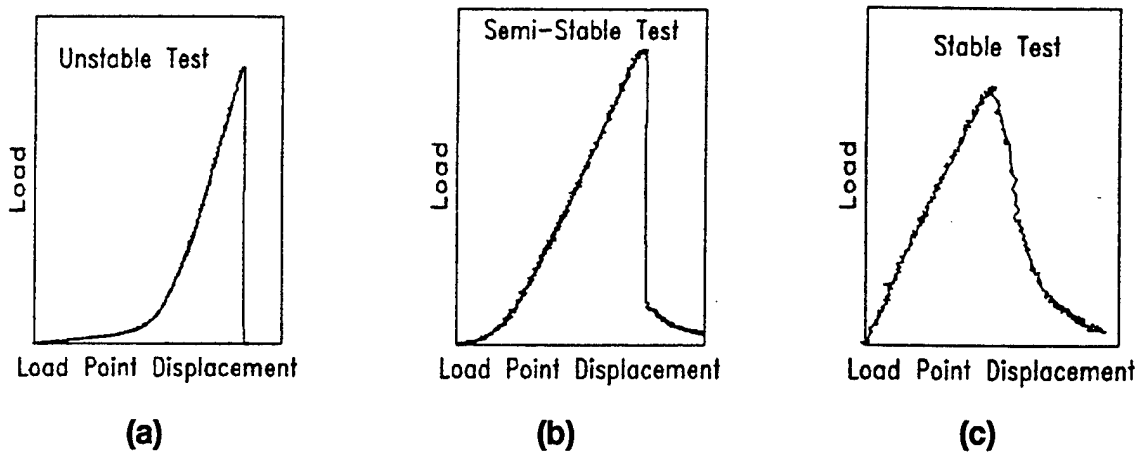
Figure 3. Typical load displacement records for (a) an unstable test, (b) a semistable test, and (c) a stable test.

For the silicon nitride (HS130) MRBB specimens, an average fracture toughness value of 2.84 ±0.13 MPa$\sqrt{m}$ was measured. This value agrees with reported literature values (Ritter et al. 1988; Baratta, Driscoll, and Katz 1974). Figure 4 shows the critical SIFs subdivided into stable and unstable results based on the appearance of the load displacement record. It can be seen that the analytically predicted threshold crack length, $(a'/W')_o = 0.59$, agrees with the experimentally observed transition from unstable to stable behavior.

8

For the alumina (AD99) MRBB specimens, an average fracture toughness value of 2.27 ± 0.10 MPa$\sqrt{m}$ was measured. Because of the lack of fracture toughness data for this alumina, three $3 \times 4 \times 40$-mm rectangular beam specimens were fabricated from the supplied round bar and critical SIFs were measured by the SEPB method (Nose and Fujii 1988). The test was performed on a screw-driven Instron testing system with 5-kN load capacity using a 0.5-kN load cell. A conventional, fully articulating, three-point bend fixture of low stiffness with a span length of 16 mm was used. The measured average fracture toughness was 2.44 ± 0.11 MPa$\sqrt{m}$, which agrees very well with the fracture toughness measured on the MRBB specimen. Figure 5 shows the critical SIF values subdivided into unstable and stable results. Again, the analytically predicted threshold crack length, $(a'/W')_o = 0.60$, divides the results into stable and unstable tests, with the exception of two data points that are stable for a somewhat shorter crack length than predicted.
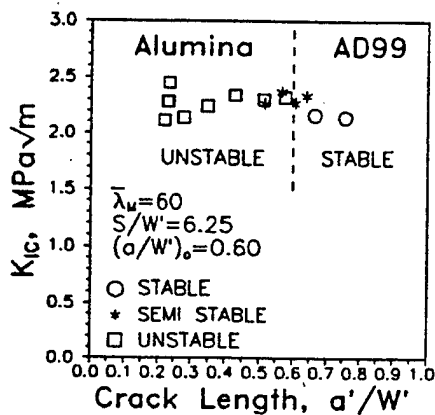
Figure 4. Measured critical stress intensity factors of the aluminia (AD99) modified round bend bars for varying precrack lengths. The predicted threshold crack length is $(a'/W')_o = 0.59$.

Figure 5. Measured critical stress intensity factors of the silicon nitride (HS130) modified round bend bars for varying precrack lengths. The predicted threshold crack length is $(a'/W')_o = 0.60$.

Alumina is typically susceptible to subcritical crack growth in air under static loading (Fett and Munz 1993). This effect would make the fracture toughness results sensitive to the displacement rate at which the test was performed, but would also promote stable crack extension for a different reason. Figure 6 summarizes the results of critical SIFs for three different displacement rates. While there appears to be no discernible effect on the mean fracture toughness value for the different loading rates, it is noteworthy that the two specimens that broke stably below the threshold crack length were tested at the lowest displacement rate. This would allow for some environmentally assisted stable crack growth to occur prior to fracture for an a/W' which is less than the predicted threshold crack length, $(a'/W')_o$.

For the silicon nitride (NC132) RTBB specimens, critical SIF values vary from a high of 4.66 MPa$\sqrt{m}$ to a low of 4.00 MPa$\sqrt{m}$. The average measured fracture toughness was 4.36 ±0.21 MPa$\sqrt{m}$. This value agrees well with reported literature values measured by several methods (Evans and Charles 1976; Salem and Shannon 1987; Anstis et al. 1981; Chantikul et al. 1981). Figure 7 shows the critical SIFs subdivided into stable and unstable results. The analytically predicted threshold crack length, $(a/W)_0 = 0.66$, agrees well with the transition observed in the experiments. One specimen with a crack length of $a/W = 0.75$ was tested in a more compliant conventional fully articulating fixture. The measured critical SIF (4.65 MPa$\sqrt{m}$) was in the same range as those obtained from the other unstable specimens. Using the more compliant fixture increased the overall machine compliance to a value much above 60. For higher machine compliance values, the stability analysis predicts a longer threshold crack length or complete instability. Thus this compliant fixture was expected to result in unstable fracture, which agreed with the observed load displacement record and the higher critical SIF.
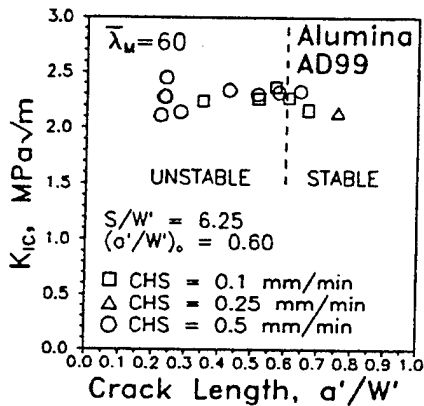
Figure 6. Measured critical stress intensity factors of the alumina (AD99) modified round bend bars grouped by displacement rates.
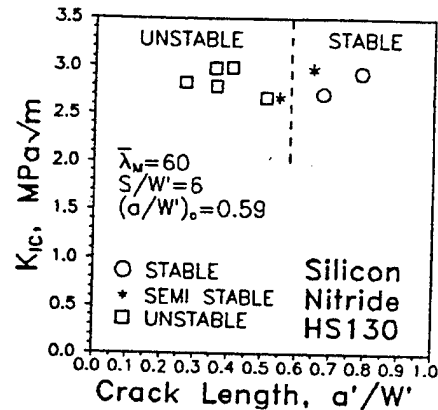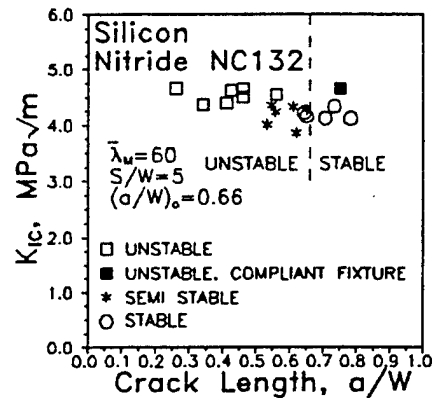
Figure 7. Measured critical stress intensity factors of the silicon nitride (NC132) rectangular bend bars for varying precrack lengths. The predicted threshold crack length is (a/W) = 0.66.

5. DISCUSSION

Baratta and Dunlay (1990) and Underwood, Baratta, and Zalinka (1991) have found that for PMMA and tungsten, the critical SIF values obtained in stable tests are lower than those obtained in unstable tests. Similar behavior has been observed for the RTBB silicon nitride (NC132) specimens in this study. No

such conclusions can be drawn based on the results obtained from the MRBB alumina (AD99) and silicon nitride (HS130) specimens. The difference between unstable and stable tests for the RTBB silicon nitride is about 10% of the average measured critical SIF. Tables 2 to 4 summarize the average measured critical SIFs of the MRBB silicon nitride (HS130) and the alumina (AD99) specimens, and the RTBB silicon nitride (NC132) specimens, respectively, grouped into unstable, semistable, and stable results based on the appearance of the load displacement record.

Table 2. Critical SIFs of Silicon Nitride (HS130) MRBB Grouped by Degrees of Stability

	Unstable	Semistable	Stable
Average Critical SIF $(MPa\sqrt{m})$	2.82 ±0.13	2.82 ±0.02	2.82 ±0.16
No. of Specimens	4	2	2
a'/W'	0.27–0.51	0.55–0.64	0.67–0.79

Table 3. Critical SIFs of Alumina (AD99) MRBB Grouped by Degrees of Stability

	Unstable	Semistable[a]	Stable
Average Critical SIF $(MPa\sqrt{m})$	2.27 ±0.10	2.31 ±0.05	2.15 ±0.01
No. of Specimens	9	4	2
a'/W'	0.22–0.58	0.52–0.64	0.67–0.76

[a] Includes specimens susceptible to subcritical crack growth.

Table 4. Critical SIFs of Silicon Nitride (NC132) RTBB Grouped by Degrees of Stability

	Unstable[a]	Semistable	Stable
Average Critical SIF $(MPa\sqrt{m})$	4.54 ±0.12	4.23 ±0.13	4.19 ±0.08
No. of Specimens	7	5	5
a/W	0.26–0.56	0.53–0.65	0.64–0.78

[a] Does not include the specimen tested in the compliant fixture.

For ceramic materials, it is typical to obtain a standard deviation of ±0.15 to 0.3 MPa$\sqrt{m}$ when fracture toughness is determined by the single edge, precracked beam (SEPB) method (Nose and Fujii 1987) regardless of the compliance of the machine and the specimen (Quinn et al. 1992). For the materials used in this MRBB geometry study, 10% would be 0.2–0.25 MPa$\sqrt{m}$, which is well within the experimental scatter of the results. To observe a noticeable difference in critical SIFs due to the instability (i.e., higher estimate of critical SIFs because of the unstable test), it would be necessary to select a material with a higher fracture toughness and a specimen with larger dimensions, so that systematic differences would not be obscured by the lack of resolution of the experiments. This lack of resolution stems largely from the large load cell with rather low resolution that is necessary to obtain the necessary stiffness. A specimen with higher fracture toughness and larger dimensions will give higher load readings, thus reducing the scatter.

A comparison of Figures 5–7 show that stability in the MRBB is obtained at a shorter crack length than for the RTBB, which is in agreement with the prediction of Figure 2. The stress intensity expression for bend bars increase rapidly as a function of dimensionless crack length, α, for $\alpha > 0.55$. Thus, for specimens with precracks long enough to be in the stable region, small errors in the crack length measurements can cause large inaccuracies in critical SIF measurements. Previous studies (Cho and Bar-On 1995; Bar-On, Baratta, and Cho, to be published) indicate that using a span-to-width ratio between 7 and 8 would lead to a shorter threshold crack length. This, in turn, would make the results less sensitive to errors in crack length measurements, thus giving more accurate fracture toughness results.

6. CONCLUSIONS

Fracture toughness tests were performed for bend bars of rectangular and modified round cross sections. The specimen precracking and test conditions were selected in such a way that a transition from unstable to stable crack extension could be observed. This transition agreed well with previously published analytical predictions and showed the MRBB to be more stable for shorter precrack lengths than the RTBB. The stable tests gave lower critical SIFs for the tougher material. A similar difference could not be discerned in the other two materials, possibly due to experimental scatter.

7. REFERENCES

Anstis, G. R., P. Chantikul, B. R. Lawn, and D. B. Marshall. "A Critical Evaluation of Indentation Techniques for Measuring Fracture Toughness: I, Direct Crack Measurements." Journal of the American Ceramic Society, vol. 64, no. 9, pp. 533–538, 1981.

ASTM E-399. "Standard Test Method for Plane-Strain Fracture Toughness of Metallic Materials." Annual Book of ASTM Standards, vol. 03.01., ASTM, Philadelphia, PA, pp. 487–511, 1989.

Bar-On, I., F. I. Baratta, and K. Cho. "Crack Stability and Its Effect on Fracture Toughness of Hot Pressed Silicon Nitride Beam Specimen." To be published in Journal of the American Ceramic Society.

Bar-On, I., J. T. Beals, G. L. Leatherman, and C. M. Murray. "Fracture Toughness of Precracked Bend Bars." Journal of the American Ceramic Society, vol. 73, no. 8, pp. 2519–2522, 1990.

Baratta, F. I. "Load-Point Compliance of a Three-Point Loaded Cracked-Notched Beam." Journal of Testing and Evaluation, vol. 16, pp. 59–71, 1988.

Baratta, F. I., G. W. Driscoll, and R. N. Katz. Ceramics for High-Performance Applications. J. J. Burke, A. E. Gorum, and R. N. Katz, editors. Brook Hill Publishing Co., Chestnut Hill, MA, 1974.

Baratta, F. I., and W. A. Dunlay. "Crack Stability in Simply Supported Four-Point and Three-Point Loaded Beams of Brittle Materials." Mechanics of Materials, vol. 10, pp. 149–159, 1990.

Bluhm, J. I. "Stability Consideration in the Generalized Three Dimensional 'Work of Fracture' Specimen." Fracture 1977, vol. 3, ICF4, Waterloo, Canada, pp. 409–417, 1977.

Bratton, R. J., and D. G. Miller. Ceramics for High Performance Applications - II. J. J. Burke, E. N. Lenoe, and R. N. Katz, editors. Brook Hill Publishing Co., Chestnut Hill, MA, 1978.

Brown, W. F., Jr., and J. E. Srawley. "Plane Strain Crack Toughness Testing of High Strength Metallic Materials." ASTM STP 410, ASTM, Philadelphia, PA, 1966.

Chantikul, P., G. R. Anstis, B. R. Lawn, and D. B. Marshall. "A Critical Evaluation of Indentation Techniques for Measuring Fracture Toughness: II, Strength Method." Journal of the American Ceramic Society, vol. 64, no. 9, pp. 539–543, 1981.

Cho, K., B. F. Hantz, IV, and I. Bar-On. "Stress Intensity Factor Calculation for a Modified Round Bend Bar by 3-D Finite Element Analysis." International Journal of Fractures, vol. 62, pp. 163–170, 1993.

Cho, K., and I. Bar-On. "Crack Stability Analysis and Fracture Toughness of Ceramic Bend Bars with a Modified Circular Cross Section." Experimental Mechanics, vol. 35, no. 2, pp. 104–111, 1995.

Clausing, D. P. "Crack Stability in Linear Elastic Fracture Mechanics." International Journal of Fractures Mech., vol. 5, pp. 211–227, 1969.

Evans, A. G., and E. A. Charles. "Fracture Toughness Determination by Indentation." Journal of the American Ceramic Society, vol. 59, no. 7–8, pp. 371–372, 1976.

Fett, T., and D. Munz. "Differences between Static and Cyclic Fatigue Effects in Alumina." Journal of Material Science Letter, vol. 12, no. 5, pp. 352–354, 1993.

MIL-STD-1942A. "Flexural Strength of High Performance Ceramics at Ambient Temperature." Military Standard 1942A, U.S. Army Materials Technology Laboratory, Watertown, MA, 1983.

Kossowsky, R. Ceramics for High-Performance Applications. J. J. Burke, A. E. Gorum, and R. N. Katz, editors. Brook Hill Publishing Co., Chestnut Hill, MA, 1974.

Lange, F. F., and J. L. Iskoe. Ceramics for High-Performance Applications. J. J. Burke, A. E. Gorum, and R. N. Katz, editors. Brook Hill Publishing Co., Chestnut Hill, MA, 1974.

Miller, D. G., C. A. Anderson, S. C. Singhal, F. F. Lange, E. S. Diaz, and R. Kossowsky. "Brittle Materials Design, High Temperature Gas Turbine Material Technology." AMMRC CTR 76-32, vol. 4, Final Report, December 1976.

Nose, T., and T. Fujii. "Strain Rate Dependence of Fracture Toughness for Ceramic Materials." In S62 Annual Meeting of Japan Ceramic Society, Nagoya, Japan, 12 May 1987.

Nose, T., and T. Fujii. "Evaluation of Fracture Toughness for Ceramic Materials by a Single-Edge-Precracked-Beam Method." Journal of the American Ceramic Society, vol. 71, pp. 328–333, 1988.

Quinn, G. D., J. Salem, I. Bar-On, K. Cho, M. Foley, and H. Fang. "Fracture Toughness of Advanced Ceramics at Room Temperature." Journal of Research of the National Institute of Standards and Technology, vol. 97, pp. 579–607, 1992.

Quinn, G. D., N. D. Corbin, and J. W. McCauley. "Thermomechanical Properties of Aluminum Oxynitride Spinel." American Ceramic Society Bulletin, vol. 63, no. 5, pp. 723-729, 1994.

Ritter, J., S. Nair, P. Gennari, and W. Dunlay. "High-Strength Reaction-Bonded Silicon Nitride." Advanced Ceramic Materials, vol. 3, no. 4, pp. 415–417, 1988.

Salem, J. A., and J. L. Shannon. "Fracture Toughness of Si_3N_4 measured with Short Bar Chevron Notched Specimens." Journal of Material Science, vol. 22, pp. 321–324, 1987.

Srawley, J. E. "Wide Range Stress Intensity Factor Expression for ASTM E-399 Standard Fracture Toughness Specimens." International Journal of Fractures, vol. 12, pp. 475–476, 1976.

Srawley, J. E., and W. F. Brown, Jr. "Fracture Toughness Testing Methods." Fracture Toughness Testing and Its Applications, ASTM STP 381, ASTM, Philadelphia, PA, pp. 133–198, 1966.

Underwood, J. H., F. I. Baratta, and J. J. Zalinka. "Fracture Toughness Tests and Displacement and Crack Stability Analyses of Round Bar Bend Specimens of Liquid-Phase Sintered Tungsten." Experimental Mechanics, vol. 31, pp. 353–359, 1991.

Warren, R., and B. Johanneson. "Creation of Stable Crack in Hard Metals Using 'Bridge' Indentation." Powder Metall., vol. 27, no. 1, pp. 211–227, 1969.

NO. OF
COPIES   ORGANIZATION

2   ADMINISTRATOR
         ATTN DTIC DDA
         DEFENSE TECHNICAL INFO CTR
         CAMERON STATION
         ALEXANDRIA VA 22304-6145

1   DIRECTOR
         ATTN AMSRL OP SD TA
         US ARMY RESEARCH LAB
         2800 POWDER MILL RD
         ADELPHI MD 20783-1145

3   DIRECTOR
         ATTN AMSRL OP SD TL
         US ARMY RESEARCH LAB
         2800 POWDER MILL RD
         ADELPHI MD 20783-1145

1   DIRECTOR
         ATTN AMSRL OP SD TP
         US ARMY RESEARCH LAB
         2800 POWDER MILL RD
         ADELPHI MD 20783-1145

         ABERDEEN PROVING GROUND

2   DIR USARL
         ATTN AMSRL OP AP L (305)

NO. OF COPIES	ORGANIZATION
1	OSD FOR RSRCH & ENGRG PENTAGON WASHINGTON DC 20301
1	DIRECTOR ATTN AMSRL OP SD TP US ARMY RESEARCH LAB 2800 POWDER MILL ROAD ADELPHI MD 20783-1197
2	ADMINISTRATOR ATTN DTIC FDAC DEFENSE TECHNICAL INFO CTR CAMERON STATION ALEXANDRIA VA 22304-6145
1	CMDR AMC ATTN AMCSCI 5001 EISENHOWER AVE ALEXANDRIA VA 22333
1	DIR ARMY RSRCH OFC ATTN INFO PROCESSING OFC PO BOX 12211 RESEARCH TRIANGLE PARK NC 27709-2211
2	CMDR US ARMY ARDEC ATTN TECH LIBRARY DR W EBIHARA PCTNY ARSNL NJ 07806
1	CMDR US ARMY TACOM ATT AMSTA TSL TECH LIBRY WARREN MI 48397-5000
1	MIAC CINDAS PURDUE UNIVERSITY 2595 YEAGER ROAD WEST LAFAYETTE IN 47905
1	CERCOM INC ATTN DR JAMES SHIH 1960 WATSON WAY VISTA CA 92083

NO. OF COPIES	ORGANIZATION
4	MATERIALS MODIFICATION INC ATTN DR T S SUDARSHAN DR CHARLIE YU MS RESHINA KUMAR DR MICHAEL LANGUELL 2929 P1 ESKRIDGE ROAD FAIRFAX VA 22031
14	WORCESTER POLYTECHNIC INST ATTN DR RONALD BIEDERMAN DR RICHARD SISSON DR ISA BAR ON (10 CP) DR MARINA PASCUCCI DR R NATHAN KATZ 100 INSTITUTE ROAD WORCESTER MA 01609
1	NATL INST OF STAND & TECHLGY ATTN MR GEORGE QUINN CERAMICS DIVISION BLDG 223 A326 GAITHERSBURG MD 02899

ABERDEEN PROVING GROUND

1	DIR, USAMSAA ATTN: AMXSY-MP
28	DIR, USARL ATTN: AMSRL-WT AMSRL-OP-CI-D, TECH LIB (2 CP) AMSRL-OP-PR AMSRL-MA-I, R. DOWDING K. CHO (20 CP) AMSRL-MA-B, T. HYNES J. SWAB G. GILDE

USER EVALUATION SHEET/CHANGE OF ADDRESS

This Laboratory undertakes a continuing effort to improve the quality of the reports it publishes. Your comments/answers to the items/questions below will aid us in our efforts.

1. ARL Report Number/Author __ARL-TR-1184 (Cho)__ Date of Report __August 1996__

2. Date Report Received _____

3. Does this report satisfy a need? (Comment on purpose, related project, or other area of interest for which the report will be used.) _____

_____

_____

4. Specifically, how is the report being used? (Information source, design data, procedure, source of ideas, etc.) ____

_____

_____

5. Has the information in this report led to any quantitative savings as far as man-hours or dollars saved, operating costs avoided, or efficiencies achieved, etc? If so, please elaborate. _____

_____

_____

6. General Comments. What do you think should be changed to improve future reports? (Indicate changes to organization, technical content, format, etc.) _____

_____

_____

_____

	Organization
CURRENT ADDRESS	Name
	Street or P.O. Box No.
	City, State, Zip Code

7. If indicating a Change of Address or Address Correction, please provide the Current or Correct address above and the Old or Incorrect address below.

	Organization
OLD ADDRESS	Name
	Street or P.O. Box No.
	City, State, Zip Code

(Remove this sheet, fold as indicated, tape closed, and mail.)
(DO NOT STAPLE)

DEPARTMENT OF THE ARMY

OFFICIAL BUSINESS

BUSINESS REPLY MAIL
FIRST CLASS PERMIT NO 0001, APG, MD

POSTAGE WILL BE PAID BY ADDRESSEE

DIRECTOR
US ARMY RESEARCH LABORATORY
ATTN AMSRL MA I
ABERDEEN PROVING GROUND MD 21005-5069